Dynamics by measurement: Aharonov's inverse quantum Zeno effect

Thomas P. Altenmüller and Axel Schenzle
Sektion Physik der Universität München, Theresienstrasse 37, 8000 München, Germany
and Max-Planck-Institut für Quantenoptik,
Ludwig-Prandtl-Strasse 10, 8046 Garching, Germany
(Received 13 July 1992)

The quantum Zeno effect is known as the inhibition of a system's reversible dynamics by frequent measurements. Aharonov and Vardi [Phys. Rev. D **21**, 2235 (1980)] proposed a scheme intimately related to the quantum Zeno effect. They showed that, by performing a dense sequence of measurements along a presumed path, the system is found to follow this—arbitrarily chosen—trajectory. The proof was based on the von Neumann projection hypothesis. In this paper we investigate whether this effect still holds if we model a realistic measurement process instead of the artificial instantaneous von Neumann collapse. We test the orientation of the Bloch vector of a two-level system using a third level and resonance fluorescence as the measuring apparatus. Therefore we are able to use a dynamical collapse governed by the three-level master equations. We show that a sequence of orientation measurements designed to monitor a particular trajectory indeed induces a dynamics exactly along this trajectory.

PACS number(s): 06.20.Dk, 42.50.Wm

I. INTRODUCTION

In classical physics, the notion of an ideal measurement implies the absence of any backaction whatsoever upon the system due to a measurement. However, in the von Neumann axiom of quantum mechanics, it is postulated that any measurement will abruptly change the state of the system under consideration, so that it will be left in an eigenstate of the measured observable. In this sense, even an ideal measurement will not leave a system undisturbed.

It is this measurement-induced projection that is behind the quantum Zeno effect. From a classical point of view, such an effect due to ideal measurements must be regarded as paradoxical. Even from the quantum-mechanical point of view, it remains obscure what kind of interaction qualifies a process to be a measurement and therefore induces such confusing consequences. In order to shed light on this problem, one must no longer adhere to the postulate of an instantaneous collapse.

It is the purpose of this paper to replace the instantaneous collapse by a detailed treatment of the physical process for a particular example. The density operator ρ and the state vector $|\psi\rangle$ are essentially only prognoses about the possible outcome of a measurement. As van Kampen clarified in a very pragmatic review, any other properties assigned to ρ and $|\psi\rangle$ are beyond physics [1]. Thus the "collapse of the wave function" is nothing but the measurement-induced update of such a prognosis. For an observer-independent discussion, we study only nonselective measurements. Hence, only the nondiagonal matrix elements of the density matrix are updated, i.e., they collapse during the measurement. The decay of the coherences deprives the system of its capability to jump into another state, and it is thereby bound to stay in a particular state. This is the "collapse of the wave function."

By treating a nonselective measurement, we can avoid single-particle trajectories. As in classical statistics, it is not meaningful to investigate one particular trajectory out of many. Therefore, the approach best suited to the measurement problem is the density-operator formalism since we can keep track of all possible outcomes of a measurement. This approach was successful in studying the quantum Zeno effect (Sec. II A).

In this paper, we examine a related effect proposed by Aharonov and Vardi [2]. They used a von Neumann collapse. It predicts a dynamical evolution of the object as a consequence of measurements along a presumed trajectory. We will describe this inverse quantum Zeno effect in Sec. II B, and propose a physical system for demonstrating this effect in Sec. III. The equations of motion are given in Sec. III A. In Sec. III B, we present a measurement procedure on the basis of the quantum master equation. We contrast our treatment with a von Neumann approach in Sec. III C. Aharonov and Vardi used the formal limit of an infinitely dense measurement sequence to lead the system along the chosen trajectory with certainty. Using a real physical process, we cannot realize this ideal limit and thus inevitably observe deviations (Sec. III D). In Sec. III E, we illustrate the inverse Zeno effect by numerical solutions of the equations of motion.

II. MEASUREMENT-INDUCED EFFECTS

A. Quantum Zeno effect

The notion of the quantum Zeno effect was first introduced by Misra and Sudarshan [3] in allusion to the paradoxon stated by Zenon of Elea in the fifth century B.C. Various aspects of the effect were discussed in a number of publications [4–10]. Generally, the quantum Zeno effect means that a system's unitary time evolution from an eigenstate of the measured observable into a superposition will be inhibited by the measurement-induced projection of the system. Furthermore, in the limit of infinitely frequent measurements, the evolution will stop

completely. The reason behind the suppression of the evolution is the absence of odd terms in time in the transition probability. Thus, if the time between measurements is small, the system will have no way to evolve substantially out of the initial state.

Cook [11] proposed an experiment to demonstrate the quantum Zeno effect using a V-level system (cf. Fig. 1). The advantage of such a system is that it offers the simplest possible object, i.e., the 1-2 transition, as well as the simplest measuring device, i.e., the 1-3 transition. In the case the system is in level 1, a laser pulse applied to the 1-3 transition will cause the system to emit fluorescence radiation, thereby indicating that the system occupies level 1. In the case there is no fluorescence despite the presence of the laser pulse, the system is in level 2.

When Itano *et al.* performed the proposed experiment [12], they found the predicted inhibition of the 1-2 transition. However, in accordance with Cook, their interpretation of the experiment used the hypothesis of an instantaneous collapse induced by the measurement process. The coherences between levels 1 and 2 were set equal to zero "by hand." With vanishing coherence there is no further evolution until coherence is newly built up by the external rf field. It is important to note that the collapse postulate is only a shortcut, roughly modeling an actual measurement process. However, it still remains open what exactly qualifies a physical process as a measurement. This can only be determined by a full quantum treatment of the interaction between system and meter. All the details of this interaction can be calculated in the case of the V-level system using the optical Bloch equations [9,10]. Instead of the collapse, the coherence was shown to decay on a time scale of order γ_3/β^2, where γ_3 is the lifetime of level 3 and β is the Rabi frequency of the optical transition.

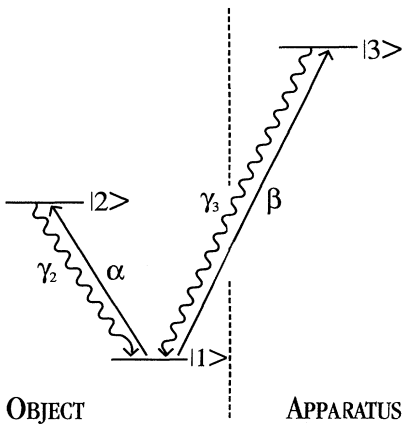

FIG. 1. V-level system. The 1-2 transition is a rf transition; α, γ_2 represent the rf Rabi frequency, resp. the natural linewidth of level 2. The 1-3 transition is driven by an intense laser field; β and γ_3 represent the laser Rabi frequency and the natural linewidth of level 3, respectively. The level separations are designated by ω_{21} and ω_{31}.

B. Inverse quantum Zeno effect

An effect intimately related to the quantum Zeno scheme was put forward by Aharonov and Vardi [2]. They showed that frequency measurement will not only bring to a halt the dynamics of a system, but also may induce a particular time evolution in a system that otherwise would stay at rest. While for the original Zeno effect, repeated measurement on the *same* state is carried out, here a sequence of measurements is performed on states that slightly change from measurement to measurement. This is done in order to monitor and verify a presumed trajectory. In the limit of a dense sequence of observations, the system is carried along an arbitrary continuous path in parameter space.

We may illustrate this using an example given by Aharonov and Vardi. Consider a spin-$\frac{1}{2}$ particle in the initial state $|\sigma_x=+1\rangle$. First, suppose there's a magnetic field along the z axis, so the spin rotates:

$$|\sigma(t)\rangle=\cos\left[\frac{\omega t}{2}\right]|\sigma_x=+1\rangle-\sin\left[\frac{\omega t}{2}\right]|\sigma_x=-1\rangle\ . \tag{1}$$

The probability of finding the system in its initial state is

$$P_{\text{initial}}=|\langle\sigma_x=+1|\sigma(t)\rangle|^2=\cos^2\left[\frac{\omega t}{2}\right]\ . \tag{2}$$

This system is clearly a candidate for the quantum Zeno effect, if only the time separation between measurements is much smaller than $2/\omega$.

In the limit of an indefinitely dense sequence of measurements, i.e., $N\to\infty$, we find

$$P_{\text{initial}}=\lim_{N\to\infty}\left[1-\left[\frac{\omega T}{2N}\right]^2\right]^N$$

$$=\lim_{N\to\infty}\exp\left[-\frac{1}{N}\left[\frac{\omega T}{2}\right]^2\right]=1\ . \tag{3}$$

Thus the motion is frozen in the spin's initial state.

Let us now define a state $|\sigma_n\rangle$:

$$|\sigma_n\rangle=\cos\alpha_n|\sigma_x=+1\rangle-\sin\alpha_n|\sigma_x=-1\rangle,$$
$$\alpha_n=\frac{\Omega T}{2}\frac{n}{N}\ . \tag{4}$$

$|\sigma_n\rangle$ describes the state of the spin after time $t_n=Tn/N$ of free evolution in an appropriate magnetic field. If we now want to find out if such a field is indeed present, we may choose to test the spin's corresponding time evolution. Thus, we calculate the probability for the spin to be in state $|\sigma(t)\rangle$ [Eq. (1)] at time t_n by projecting $|\sigma(t)\rangle$ onto $|\sigma_n\rangle$. If—as we conjecture—$\Omega=\omega$, then the spin is always projected onto itself. Therefore we do not interfere with the spin's free evolution.

Now suppose the magnetic field is switched off. We still may ask for the probability of finding the spin in state $|\sigma_n\rangle$ provided the spin was in state $|\sigma_{n-1}\rangle$ before this measurement:

$$P_{n-1\to n}=|\langle\sigma_n|\sigma_n-1\rangle|^2=\cos^2\left[\frac{\Omega T}{2N}\right]. \tag{5}$$

An observer unaware of the absence of the field may still assume that the spin precesses with Ω and therefore try to monitor the presumed precession. Thus he performs an entire sequence of measurements $\{|\sigma_m\rangle\langle\sigma_m|\}_{m=1,\cdots,N}$. The conditional probability of finding the spin in $|\sigma_N\rangle$, provided it was initially in $|\sigma_x=+1\rangle$, is a product of the P_n's:

$$P_{n=0\to N}=\prod_{n=0}^{N}P_n=\left[\cos\left[\frac{\Omega T}{2N}\right]\right]^{2N}. \tag{6}$$

For large N, we obtain

$$P_{n=0\to N}=\exp\left[-\frac{1}{N}\left[\frac{\Omega T}{2}\right]^2\right]. \tag{7}$$

In the limit of an infinitely dense sequence, we find again

$$\lim_{N\to\infty}P_{n=0\to N}=1\ . \tag{8}$$

This means that the spin, even without any magnetic field, is found to precess. This rotation, however, is exclusively due to the observer's prejudice in favor of a particular trajectory and his design of the measurements along this trajectory. Moreover, the observer can choose whatever trajectory he conceives to be reasonable and "verify" it by an appropriate sequence of α_n's in Eq. (4). From a classical point of view, this is clearly a grotesque consequence of the standard quantum-mechanical measurement theory. Hence the question arises whether this is only due to the artificial von Neumann postulate or whether this effect still holds when a realistic measurement process is considered.

III. PULLING THE BLOCH VECTOR

We would like to combine the inverse quantum Zeno effect with the idea of a dynamical collapse. A system demonstrating the inverse quantum Zeno effect must meet several requirements. First, there has to be a clear division in object and apparatus. Second, the object must be described by at least two orthonormal states. Third, the meter must be sensitive to any chosen superpositions of the object states. A simple system meeting these requirements is the V-level system in combination with a particular measurement procedure. As for the quantum Zeno effect, the 1-3 transition serves as apparatus. However, this time we are not looking for the population on the 1-2 transition alone, but we measure an arbitrary orientation of the corresponding Bloch vector.

A. Equations of motion

The 1-2 transition (the object) is coupled to a rf field, and the 1-3 transition (the apparatus) is coupled to an intense pulsed laser field with resonant frequency in the optical region. For the present purpose, both fields are classical. Furthermore, all transitions are coupled to the quantized multimode vacuum. After employing the standard rotating-wave approximation and a transformation to the rotating frame (e.g. [13]), we perform the usual transition to irreversible quantum mechanics by eliminating all degrees of freedom of the heat bath (e.g. [14]). Thereby we arrive at a master equation containing only variables of the V-level system.

Instead of formulating the equations of motion for the object system as ρ_{ij}, $i,j=1,2$, it is more illustrative to use the Bloch vector representation (e.g., [13]):

$$u=\rho_{12}+\rho_{21},\quad v=-i(\rho_{12}-\rho_{21}),\quad w=\rho_{22}-\rho_{11}\ . \tag{9}$$

So, finally, the equations of motion read

$$\begin{aligned}
\frac{d}{dt}u&=-\alpha\sin\phi w-(\omega_{21}-\omega)v-\frac{\gamma_2}{2}u-i\beta(\rho_{23}-\rho_{32})\ ,\\
\frac{d}{dt}v&=\alpha\cos\phi w+(\omega_{21}-\omega)u-\frac{\gamma_2}{2}v+i\beta(\rho_{23}+\rho_{32})\ ,\\
\frac{d}{dt}w&=\alpha\sin\phi u-\alpha\cos\phi v-\gamma_2(w-\rho_{33}+1)\\
&\quad+i\beta(\rho_{13}-\rho_{31})\ ,\\
\frac{d}{dt}\rho_{33}&=i\beta(\rho_{13}-\rho_{31})-\gamma_3\rho_{33}\ ,\\
\frac{d}{dt}\rho_{23}&=-i\frac{\beta}{4}(v+iu)+i\frac{\alpha}{2}\rho_{13}-\frac{\gamma_2+\gamma_3}{2}\rho_{23}\ ,\\
\frac{d}{dt}\rho_{13}&=i\frac{\alpha}{2}\rho_{23}+i\frac{\beta}{2}[\rho_{33}-\tfrac{1}{2}(1-w)]-\frac{\gamma_3}{2}\rho_{13}\ .
\end{aligned} \tag{10}$$

Here, ω_{21} is the level splitting between levels 1 and 2, ω is the frequency, ϕ the phase, and α the Rabi frequency of the rf field. The spontaneous decay rate γ_2 of level 2 can safely be neglected for an rf transition. ω_{31} is the resonant laser frequency, β the Rabi frequency of the optical transition, and γ_3 the spontaneous decay rate from level 3.

It is useful for the following to recall that the dynamics of the undisturbed two-level system resembles a spin precessing in an effective field:

$$\frac{d}{dt}\mathbf{R}=\mathbf{R}\times\mathbf{B}\ , \tag{11}$$

with

$$\mathbf{R}={}^t(u,v,w)\ , \tag{12}$$

$$\mathbf{B}={}^t(\alpha\cos\phi,\ \alpha\sin\phi,\ -(\omega_{21}-\omega))\ . \tag{13}$$

The effective field $\mathbf{B}$ depends on the resonance condition and the phase of the applied rf field. In the following, we will choose $\omega=\omega_{21}$ (resonance), thus causing the effective field $\mathbf{B}$ to lie in the u-v plane with angle ϕ to the u axis.

The interaction of the object with the apparatus in Eqs. (10) will lead to the dynamical collapse of the coherences of the 1-2 transition, i.e., $u,v\to 0$, if β and γ_3 are by orders of magnitude greater than α [9,10]. So the dynamics governed by Eqs. (10) can be summarized as follows: While the rf field causes a slow reversible rotation of the Bloch vector on a cone, the laser pulse will irreversibly project the Bloch vector to the w axis within a very short time.

B. Realization of phase and inversion measurement

We want to exploit the V-level's dynamics for a combined measurement of phase and inversion of the object system. Phase and inversion are described by the Bloch vector's azimuthal and polar angle:

$$\phi_{21}=-\arctan\left[\frac{u}{v}\right], \tag{14}$$

$$\theta_{21}=\arctan\left[\frac{(u^2+v^2)^{1/2}}{w}\right]. \tag{15}$$

(The minus sign is due to the angle ϕ_{21} being taken from the negative v axis.)

In Cook's original quantum Zeno scheme, the system is subjected to an intense laser pulse, causing the 1-3 transition to emit fluorescence photons depending on the inversion of the 1-2 transition. This measurement answers the question "Is $w=+1$" or equivalently "$\theta_{21}=0$?". If the answer is "yes," there is no fluorescence, otherwise we could detect fluorescence photons.

However, we are interested in a more general question: "Is $\phi_{21}=\phi$ and $\phi_{21}=\theta$?", where ϕ,θ can be arbitrarily chosen by the observer. Unfortunately, using the V-level scheme, it is only possible to measure inversion. However, an appropriate rf pulse can bring the Bloch vector into the w direction, where it can be measured by a laser pulse according to Cook's scheme. Subsequently, it is rotated back to its initial orientation. Altogether, this requires a 2π rf pulse for measuring purposes. Because the phase ϕ is kept constant during the rf pulse, a 2π pulse will not change the system.

Now, suppose the Bloch vector initially points in the negative v direction ($\phi_{21}=0$, $\theta_{21}=\pi/2$). If we choose the effective field to lie in the u direction ($\phi=0$), then a $\pi/2$ pulse will rotate the Bloch vector into the positive w axis. Applying a short laser pulse will verify this orientation by the absence of a fluorescence signal. A subsequent $(3/2)\pi$ pulse will reverse the effects of the $(1/2)\pi$ pulse, so there are no net effects of the rf field.

However, if the initial orientation slightly differs from the v direction, the $\pi/2$ pulse will leave the Bloch vector tilted with respect to the w axis. The laser pulse nevertheless projects the vector into the w axis, and the subsequent $(3/2)\pi$ pulse rotates it into the v direction no matter what the initial orientation was. So if we only guessed the initial orientation and defined the rf-field parameters correspondingly, we always "verify" this guess. Given that our initial guess was good but not accurate, the odds are against a detection of our slight error, because it is highly improbable that, under these conditions, fluorescence will occur, indicating the answer "no."

Next we formulate a general procedure for measuring an arbitrary orientation of the Bloch vector. The initial parameters are

$$\phi_{21}^0=-\arctan\left[\frac{u_0}{v_0}\right],\quad \theta_{21}^0=\arctan\left[\frac{(u_0^2+v_0^2)^{1/2}}{w_0}\right],$$
$$L_0=(u_0^2+v_0^2+w_0^2)^{1/2}, \tag{16}$$

where L_0 is the length of the Bloch vector. This explicit definition includes the possibility of the measurements not being the first one, i.e., the length of the Bloch vector may have been reduced before, i.e, $L_0<1$.

The measurement procedure can be summarized as follows:

(i) θ rf pulse: During time θ/α, **R** rotates on a cone with aperture $2\arccos\{\sin\theta_{21}^0\cos[\pi/2-(\phi-\phi_{21}^0]\}$ around **B**. As defined above, ϕ is the angle between **B** and the u axis. This leaves **R** inclined with respect to the w axis.

(ii) Laser pulse: Due to the interaction with the laser field, u,v decay to zero very quickly. This projects **R** to the w axis and leads to a loss of length.

(iii) $2\pi-\theta$ rf pulse: This pulse continues the rotation of **R**, now on a disc perpendicular to **B**. Since θ changed also in (ii), the rotation will not lead back to θ_{21}^0.

As calculated in the Appendix, in the limit of complete reduction due to the laser pulse, the above procedure leads to

$$\mathbf{R}=L_0[\cos(\phi-\phi_{21}^0)\sin\theta\sin\theta_{21}^0+\cos\theta\cos\theta_{21}^0]\times\begin{bmatrix}\sin\theta\sin\phi\\ \sin\theta(-\cos\phi)\\ \cos\theta\end{bmatrix}. \tag{17}$$

Originally, ϕ was the field's phase, i.e., the angle between **B** and the positive u axis. Since after the above measurement procedure, **R** and **B** are perpendicular, ϕ_{21} is found to be ϕ.

The crucial point here is that the Bloch vector points in the direction given by the observer's first guess (i.e., arbitrarily chosen ϕ and θ). If we perform a sequence of measurements on the orientation of the Bloch vector at times t_n, we will find **R** pointing in the direction given by functions $\phi(t_n)$ and $\theta(t_n)$ after each measurement. Hence **R** is pulled along whatever trajectory the experimenter chooses to test. The system's path differs from similar trajectories due to a reversible evolution (e.g., adiabatic following) in one important aspect: Since the measurements "pin" it to $(\phi(t),\theta(t))$, it is in a sense "classical." The system's evolution is not a coherent evolution from one state into another, as it is for reversible schemes. It is interrupted by incoherent processes, so that the system's dynamic—at least in the limit of continuously monitoring—resembles more an incoherent classical motion in the sense that the path does not interfere with neighboring paths.

Since $[\cos(\phi-\phi_{21}^0)\sin\theta\sin\theta_{21}^0+\cos\theta\cos\theta_{21}^0]\leq 1$, the Bloch vector shrinks slightly by each measurement, i.e., the state is turned into a statistical mixture. This means that we keep track of all possible paths an individual member of an ensemble may evolve for a given sequence $(\phi(t_n),\theta(t_n))$. The loss of length of **R** is studied more quantitatively in Sec. III D. It turns out that, for a sufficiently dense sequence, essentially one path, namely the one prescribed by $(\phi(t_n),\theta(t_n))$, is realized.

The sequence of measurements requires $\phi(t)$ to be a stepped function, which is constant during the rf pulses and only varies between the pulses. However, if $\phi(t)$ is allowed to change during the rf pulse, an additional re-

versible effect comes into play, i.e., adiabatic following. In order not to confuse the issue, we will emphasize the measurement-induced phenomenon by using a stepped function instead, where adiabatic following does not occur. In any case, the effects of adiabatic following are weak and do not change visibly the outcome.

As was already pointed out in the end of Sec. II B from the point of view of measurement theory, the dragging of the Bloch vector by ideal measurements is irritating. Yet, modeling the measurement by a physical process, we show that the pulling effect is a straightforward consequence of the system's irreversible dynamics. It is the very purpose of this paper to show the simple physics behind the strange implications of the standard measurement theory.

C. Using the von Neumann approach

For comparison, it is instructive to investigate the measurement process using the von Neumann approach: The state of the system is reduced in an arbitrary orthonormal base. The above measurement concept for the V-level system must yield the same result in the limit of intense laser fields and fast decay of level 3.

A Bloch vector of length 1, with azimuthal angle ϕ_{21} and polar angle θ_{21}, represents an object state

$$|\phi_{21},\theta_{21}\rangle = e^{i\phi_{21}}\sin\left[\frac{\theta_{21}}{2}\right]|1\rangle + i\cos\left[\frac{\theta_{21}}{2}\right]|2\rangle \tag{18}$$

up to an arbitrary phase. The Hilbert space of possible states is spanned by, e.g.,

$$\begin{aligned}|\phi,\theta\rangle &= e^{i\phi}\sin\left[\frac{\phi}{2}\right]|1\rangle + i\cos\left[\frac{\theta}{2}\right]|2\rangle\ ,\\ |\phi-\pi,\pi-\theta\rangle &= e^{i(\phi-\pi)}\sin\left[\frac{\pi-\theta}{2}\right]|1\rangle + i\cos\left[\frac{\pi-\theta}{2}\right]|2\rangle\ .\end{aligned} \tag{19}$$

This base represents two Bloch vectors of length 1, one pointing in direction (ϕ,θ), the other in the opposite direction. The initial conditions before the measurement are

$$\begin{aligned}u_0 &= \sin\theta_{21}^0\sin\phi_{21}^0,\quad v_0 = \sin\theta_{21}^0(-\cos\phi_{21}^0)\ ,\\ w_0 &= \cos\theta_{21}^0\ ,\end{aligned} \tag{20}$$

or, equivalently,

$$|\phi_{21}^0,\theta_{21}^0\rangle = e^{i\phi_{21}^0}\sin\left[\frac{\theta_{21}^0}{2}\right]|1\rangle + i\cos\left[\frac{\theta_{21}^0}{2}\right]|2\rangle\ . \tag{21}$$

In the base of Eqs. (19), the initial state reads

$$|\phi_{21}^0,\theta_{21}^0\rangle = c_{\phi\theta}|\phi,\theta\rangle + c_{\phi-\pi,\pi-\theta}|\phi-\pi,\pi-\theta\rangle\ , \tag{22}$$

with

$$\begin{aligned}c_{\phi\theta} &= e^{i(\phi_{21}^0-\phi)}\sin\left[\frac{\theta}{2}\right]\sin\left[\frac{\theta_{21}^0}{2}\right] + \cos\left[\frac{\theta}{2}\right]\cos\left[\frac{\theta_{21}^0}{2}\right]\ ,\\ c_{\phi-\pi,\pi-\theta} &= -e^{i(\phi_{21}^0-\phi)}\cos\left[\frac{\theta}{2}\right]\sin\left[\frac{\theta_{21}^0}{2}\right] + \sin\left[\frac{\theta}{2}\right]\cos\left[\frac{\theta_{21}^0}{2}\right]\ .\end{aligned} \tag{23}$$

The density-matrix representation for the initial state in the base Eqs. (19) is

$$\begin{aligned}\rho^0 &= |\phi_{21}^0,\theta_{21}^0\rangle\langle\phi_{21}^0,\theta_{21}^0|\\ &\leftrightarrow \begin{bmatrix} |c_{\phi\theta}|^2 & c^*_{\phi-\pi,\pi-\theta}c_{\phi\theta} \\ c^*_{\phi\theta}c_{\phi-\pi,\pi-\theta} & |c_{\phi-\pi,\pi-\theta}|^2 \end{bmatrix}\ .\end{aligned} \tag{24}$$

Modeling a nonselective measurement, whether the system is in state $|\phi,\theta\rangle$ or not, we obtain

$$\begin{aligned}\rho &= P_{\phi\theta}\rho_0 P_{\phi\theta} + P_{\phi-\pi,\pi-\theta}\rho_0 P_{\phi-\pi,\pi-\theta}\\ &\leftrightarrow \begin{bmatrix} |c_{\phi\theta}|^2 & 0 \\ 0 & |c_{\phi-\pi,\pi-\theta}|^2 \end{bmatrix}\ ,\end{aligned} \tag{25}$$

where

$$\begin{aligned}P_{\phi\theta} &= |\phi,\theta\rangle\langle\phi,\theta|\ ,\\ P_{\phi-\pi,\pi-\theta} &= |\phi-\pi,\pi-\theta\rangle\langle\phi-\pi,\pi-\theta|\ ,\end{aligned} \tag{26}$$

i.e., the nondiagonal elements in the measurement base are collapsed. To illustrate the effects of the measurement on the Bloch vector representation, we transform back to u,v,w. This yields

$$u = a\sin\theta\sin\phi,\quad v = a\sin\theta(-\cos\phi),\quad w = a\cos\theta\ , \tag{27}$$

with

$$a = [\cos(\phi-\phi_{21}^0)\sin\theta\sin\theta_{21}^0 + \cos\theta\cos\theta_{21}^0]\ . \tag{28}$$

Thus the measurement-induced collapse leads to a Bloch vector pointing in the ϕ,θ direction. Comparison of this result with Eq. (17) shows complete agreement, indicating that the procedure presented in Sec. III B perfectly models an ideal measurement. On the other hand, since $a \leq 1$, the length of the Bloch vector shrinks due to the contribution of $|\phi-\pi,\pi-\theta\rangle$ to the initial state. However, as is shown in Sec. III D, if $(\phi_{21}^0-\phi)$ and $(\theta_{21}^0-\theta)$ are small enough, a is essentially 1.

D. Shrinking of the Bloch vector

Geometrical considerations yield

$$a = \cos\Delta\phi\cos\Delta\theta + O(\Delta\phi^4)\ , \tag{29}$$

instead of Eq. (28). Here, $\Delta\phi = \phi_{21}^0 - \phi$, but $\Delta\theta = \theta'^0_{21} - \theta$, where θ'^0_{21} is the projection of θ_{21}^0 on a plane perpendicular to **B**, since only θ'^0_{21} and θ refer to the same meridian of the Bloch sphere. Although $a = \cos\Delta\phi\cos\Delta\theta$ is

geometrically more appealing, it is only approximately valid [Eq. (29)], since projection in a two-dimensional Hilbert space does not correspond exactly to projection in the three-dimensional Bloch sphere.

Loss of length may be as small as desired by simply taking $\phi(t)$ and $\theta(t)$ as functions that hardly change from pulse to pulse. Let τ be the time between each pair of measurements. Clearly, $\tau > 2\pi/\alpha$ must be valid. For instance, suppose we set

$$\phi(t)=v_\phi \tau n, \quad \theta(t)=v_\theta \tau n \ , \quad t\in[(n-1)\tau, n\tau] \ . \tag{30}$$

Thus $\Delta\phi=v_\phi\tau$ and $\Delta\theta=v_\theta\tau$. Choosing appropriate values for v_ϕ and v_θ renders $\Delta\phi,\Delta\theta \ll 1$. When we perform a sequence of N measurements during time $N\tau$, we drag the Bloch vector over ranges $\Delta_\phi=N\Delta\phi$ and $\Delta_\theta=N\Delta\theta$; meanwhile, the Bloch vector shrinks by

$$a^N=\cos^N\Delta\phi\cos^N\Delta\theta\simeq\exp\left[-\frac{1}{2N}(\Delta_\phi^2+\Delta_\theta^2)\right] \ . \tag{31}$$

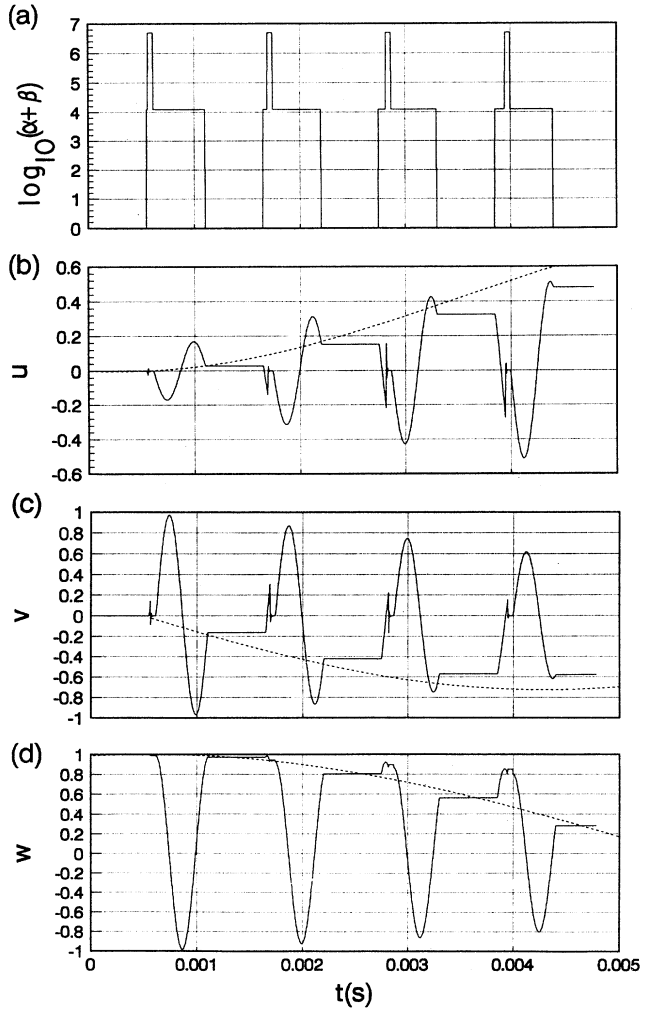

FIG. 2. (a) First four pulses of a measurement sequence. At times $t=(2n-1)\tau$, $n=1,\ldots,N$, $\tau=5.5\times10^{-4}$ s, a rf pulse is started. This rf pulse is interrupted at $t=(2n-1)\tau+\tau_{\rm rf}\theta/2\pi$, $\tau_{\rm rf}=0.9\tau$. During $\Delta t=0.1\tau$, an intense laser pulse sets in. At $t=(2n-1)\tau+\tau_{\rm rf}\theta/2\pi+\Delta t$, the laser pulse stops and the rf pulse continues until $t=2n\tau$. The solid lines in (b), (c), and (d) show the u, v, and w components, respectively; the dashed line in each panel shows a nominal curve for the case of loss-free evolution. The parameters used were $v_\theta=100\pi$ rad/s, $v_\phi=50\pi$ rad/s, $\gamma_3=10^6\ {\rm s}^{-1}$, $\beta=5\times10^6$ Hz, $\alpha=12\,566$ Hz.

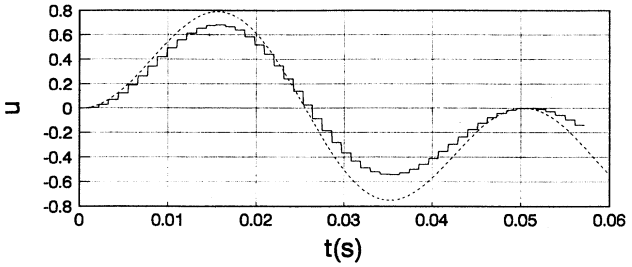

FIG. 3. Evolution of the u component for high v_θ, v_ϕ for an entire measurement sequence. The parameters were as in Figs. 2, except for $v_\theta=40\pi$ rad/s and $v_\phi=20\pi$ rad/s. Note the high losses in the deviation from the nominal curve.

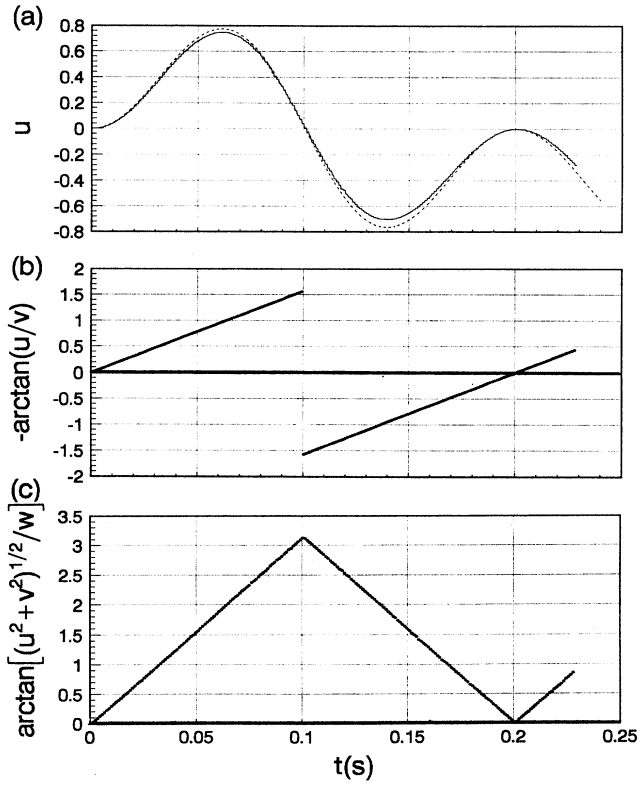

FIG. 4. (a) As Fig. 3, except for $v_\theta=10\pi$ rad/s and $v_\phi=5\pi$ rad/s. The losses are smaller than in Fig. 3, but the total time is longer. (b) The dotted line shows $\phi_{21}=-\arctan(u/v)$, the resulting azimuthal angle of the Bloch vector. Each dot represents the angle after the measurement. The angle neatly follows the deterministic sequence $(v_\phi(t_n))$. (c) The polar angle $\theta_{21}=\arctan[(u^2+v^2)^{1/2}/w]$ is shown. It follows the deterministic sequence $(v_\theta(t_n))$. In all figures, the same parameters were used as in Fig. 2.

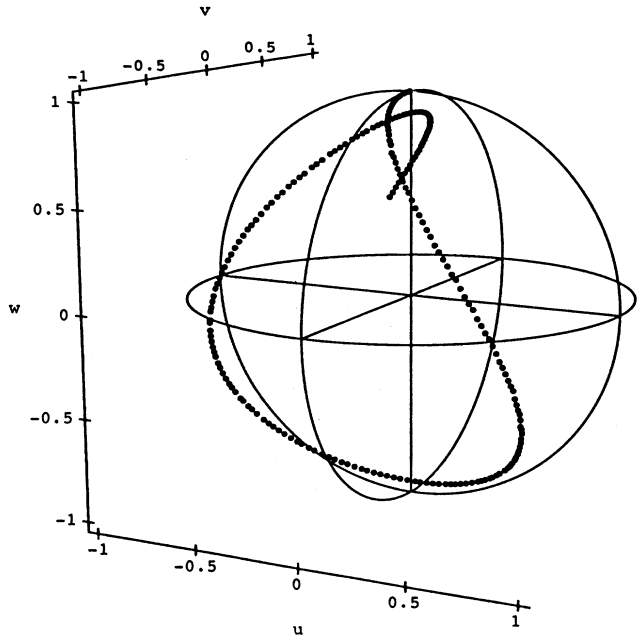

FIG. 5. Trajectory of the tip within the Bloch sphere. The drag velocities were $v_\theta = 10\pi$ rad/s and $v_\phi = 5\pi$ rad/s.

The total loss $(1-a^N)$ is monotonically decreasing with N, the number of measurements, while the total measurement time $T = N\tau$ is increasing linearly with N. The limit $N \to \infty$, $a^N \to 1$ is practically impossible, since this would take infinite measurement time. This means that, for the actual experimental realization of the inverse Zeno effect,

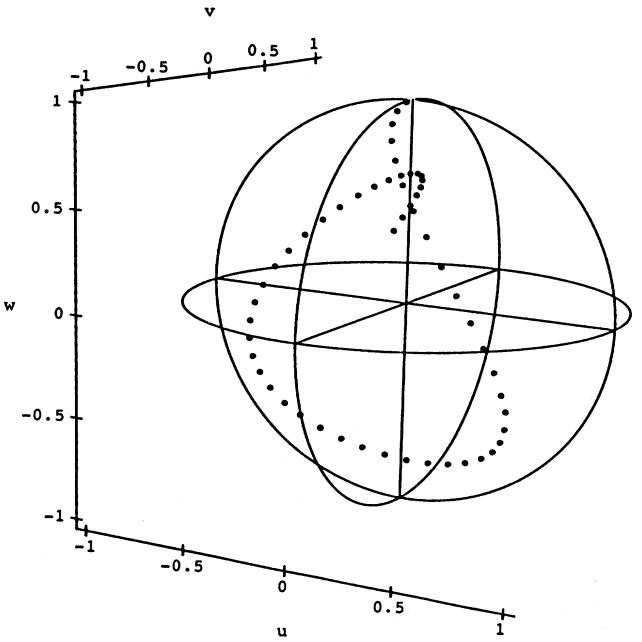

FIG. 6. As Fig. 5, but for $v_\theta = 40\pi$ rad/s and $v_\phi = 20\pi$ rad/s. Since this is much faster than in Fig. 5, the losses are higher, and total time is shorter.

there is a small but nonvanishing probability that the system resists fitting in the observer's prejudice. In the case of the V-level system, the rare event of a deviation from the prescribed trajectory would be indicated by the emission of fluorescence radiation from the 1-3 transition.

E. Numerical solution

In the following, we show and comment on results of a numerical study of Eqs. (10). The measurement sequence is governed by the two functions Eqs. (30). In principle, any other function of t will do; however, we choose stepped functions in order to logically separate measurement-induced effects from all other possible dragging influences.

In the present examples, we always choose a ratio $v_\theta / v_\phi = 2$. The initial conditions is $\mathbf{R} = {}^t(0,0,1)$.

The pulses are shown in Fig. 2(a). Note how the laser pulse is advancing slowly within the rf pulse from pulse to pulse. In Fig. 2(b), the evolution of the u component

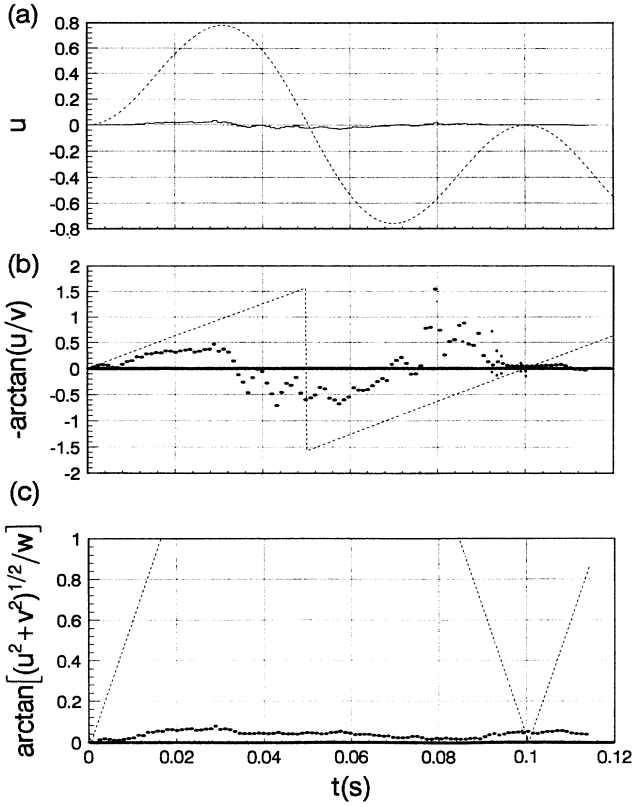

FIG. 7. Lines of small laser Rabi frequency ($\beta = 1.1 \times 10^4$ Hz, $v_\theta = 20\pi$ rad/s), $v_\phi = 10\pi$ rad/s. (a) The solid line shows the evolution of the u component with almost no reduction at all. The nominal line represents the completely reduced, loss-free case. (b) and (c) show ϕ_{21} and θ_{21} and their nominal values for complete reduction. Note that ϕ_{21} is less sensitive to the incompleteness of the reduction, while θ_{21} is almost not dragged at all. This shows that a phase is changed more easily by external fields than by an inversion, because changing the inversion requires energy exchange.

of the Bloch vector is displayed. Note the oscillatory decay to $u=0$ during the laser pulse. The dashed line designates a nominal curve, which should be followed by the components of **R** in the case of an infinitely dense sequence. In Figs. 2(c) and 2(d), the corresponding evolution of v and w are shown as solid lines. Since in Figs. 2(a–c), $v_\phi=50\pi$ rad/s and $v_\theta=100\pi$ rad/s were chosen rather fast, there are high losses. Approximately, the loss per pulse is $(1-\cos v_\phi 2\tau \cos v_\theta 2\tau)\simeq 7.3\%$.

In the following figures, the rapid evolution during the pulses is suppressed and we only show the orientation of the Bloch vector between measurements. This is done for graphical clarity.

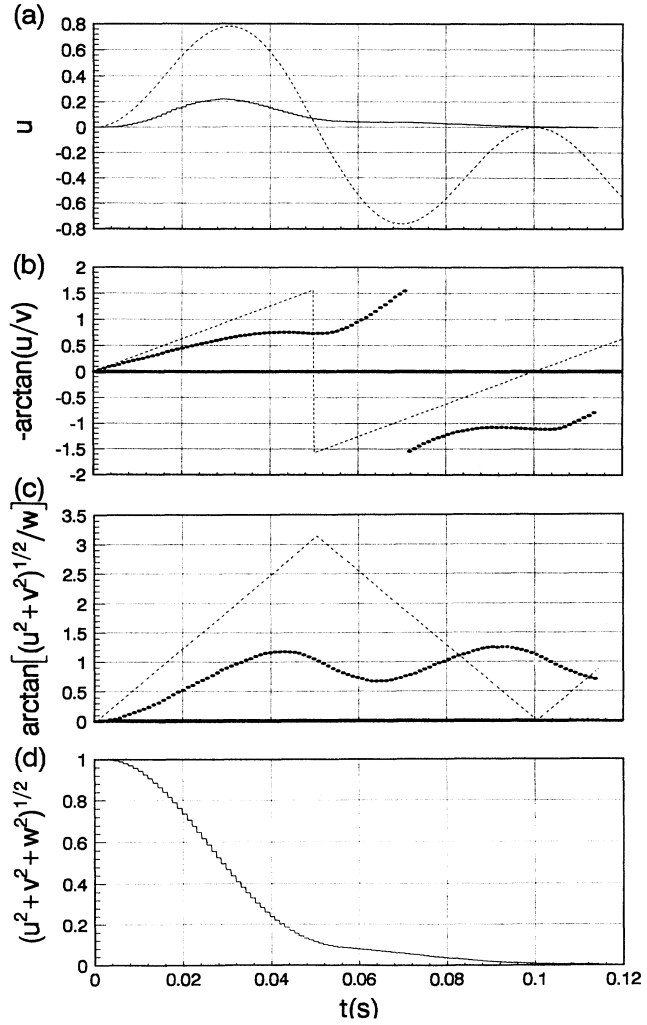

FIG. 8. Regime of partial reduction ($\beta=6\times10^4$ Hz, $v_\theta=20\pi$ rad/s, $v_\phi=10\pi$ rad/s). (a) shows the u component's evolution and its nominal values (complete reduction, loss-free). (b) and (c) show ϕ_{21} and θ_{21} and their nominal values. There is dragging, but it is retarded and incomplete. (d) displays the length of the Bloch vector in the course of measurements. As was pointed out in the text, the loss is greatest when the Bloch vector reaches the equatorial plane and is smallest when it approaches the polar regions [cf. (c)].

Figures 3 and 4(a) display the evolution of the u component for two different "velocities" v_θ and v_ϕ. The range of θ and ϕ is somewhat more than $(0\ldots2\pi)$ [respectively $(0\ldots\pi)$]. Note that the smaller v_θ and v_ϕ are, the smaller is the loss after the entire sequence, but the longer the total time. For example, consider the situation at $\theta=3\pi/2$ [respectively, $\phi=3\pi/4$]: The total loss up to this point is $(1-a^N)$, a^N given by Eq. (31):

$$a^N=[\cos(v_\theta 2\tau)\cos(v_\phi 2\tau)]^N \simeq \exp\left\{-\frac{1}{2N}\left[\left[\frac{3}{4}\pi\right]^2+\left[\frac{3}{2}\pi\right]^2\right]\right\}, \quad N=\frac{3\pi}{4}\frac{1}{v_\theta\tau}. \tag{32}$$

This yields, in Fig. 3, $a^N=0.66$ $(N=34)$, and in Fig. 4(a), $a^N=0.90$ $(N=136)$. The loss for each component of the Bloch vector is the same.

Figures 4(b) and 4(c) show the polar angles of **R**, which are newly set by each measurement process. Obviously $\phi_{21}=\arctan(u/v)$ and $\theta_{21}=\arctan[(u^2+v^2)^{1/2}/w]$ neatly follow the prescribed trajectory. Figures 5 and 6 show the trajectory in a three-dimensional plot of the Bloch sphere for slow (Fig. 5) and fast dragging (Fig. 6).

The very success of a measurement depends crucially on the degree of reduction of u and v during the laser pulse. For a complete reduction, a minimal Rabi frequency for the laser light is necessary. To obtain complete reduction, we have used $\beta=5\times10^6$ Hz for all examples. Now we want to vary β to see the effects of a partial reduction. In the limit of a very small or vanishing Rabi frequency, the Bloch vector will rotate during the rf pulse, but there will be neither losses nor dragging. If observed only between the pulses, the Bloch vector will not move on average; there will be only a slight trembling of the tip around its initial position. An example in this regime is shown in Figs. 7(a)–7(c).

With increasing β, the regime of partial reduction is reached. Poor dragging and high losses are the main features [Figs. 8(a)–8(d)]. This is somewhat surprising since the losses are much higher than for an example with the same dragging velocity but complete reduction. The explanation is as follows. Partial reduction means that u,v do not decay to zero during the laser pulse, but stop before. Thus, the subsequent rf pulse cannot rotate the Bloch vector in the desired nominal direction. So the dragging is incomplete. The next rf pulse rotates the Bloch vector into the vicinity of the w axis, only if the previous collapse has led to complete dragging. Since this was not the case, the Bloch vector's tip is farther from the w axis. Because the loss is proportional to the distance from tip to w axis, it is greater than in the case of complete reduction. The distance is equal to $(u^2+v^2)^{1/2}\propto\sin\theta_{21}$. So, for the Bloch vector in the equatorial plane, the losses are maximum; in the polar regions, they are minimum; see Figs. 8(c) and 8(d).

IV. CONCLUSION

In classical mechanics, measurement or observation does not interfere with the particle's dynamic evolution in space and time. A measurement merely extracts information on position and momentum without disturbing the system's path in any way. In quantum mechanics, observation is a much more subtle phenomenon, since the measurement inevitably leaves a trace on the system's dynamic evolution, as delicate and weak as the interaction may be. The concept of the Zeno effect, and more so, the inverse effect discussed here, demonstrates that in the case of frequently repeated measurements, results are produced that must be considered absurd from a classical point of view. While the measurement procedure of the normal Zeno effect brings the dynamics to a complete halt when a particular physical property is measured in rapid succession, the inverse effect seems even more obscure. When the meters are positioned and timed in such a way to monitor a particle along a presumed path, the experimenter will inevitably find the particle on any path he chooses to test, although otherwise, without such a test, the particle would remain undisturbed in its initial state.

In this paper we have demonstrated that such a startling phenomenon is not a mere illusion brought about by an overidealized measurement concept, but can be observed experimentally. By tracing the wave-function collapse back to its physical origin, i.e., the interaction of the object with a realistic quantum-mechanical meter, the collapse becomes a natural and continuous part of the systems dynamics. To illustrate how this effect can be seen in a laboratory experiment, we show in detail how the tip of the Bloch vector is dragged along an arbitrary path on the surface of the Bloch sphere by performing a sequence of measurements on the Bloch vector orientation. By abandoning the collapse hypothesis and replacing it by an irreversible physical interaction, it becomes possible to describe the time evolution of the observed system in quantitative detail, which only in a limiting case agrees with the results of the artificial collapse procedure.

APPENDIX

It is a simple task to calculate the dynamics of the V-level system from Eqs. (10), when one takes advantage of the very fast decay of the u and v due to the intense laser pulse. In this case, Eqs. (10) simplify to Eqs. (11). Solving these equations for a general initial condition $\mathbf{R}_0={}^t(u_0,v_0,w_0)$ gives

$$\begin{bmatrix} u(t) \\ v(t) \\ w(t) \end{bmatrix} = \begin{bmatrix} u_0(\cos^2\phi+\sin^2\phi\cos\alpha t)+v_0\sin\phi\cos\phi(1-\cos\alpha t)-w_0\sin\phi\sin\alpha t \\ u_0\sin\phi\cos\phi(1-\cos\alpha t)+v_0(\sin^2\phi+\cos^2\phi\cos\alpha t)+w_0\cos\phi\sin\alpha t \\ u_0\sin\phi\sin\alpha t-v_0\cos\phi\sin\alpha t+w_0\cos\alpha t \end{bmatrix} . \tag{A1}$$

Now we perform the measurement procedure proposed in Sec. III B. The initial condition before the measurement is

$$\mathbf{R}_0=L_0\begin{bmatrix} \sin\theta_{21}^0\sin\phi_{21}^0 \\ \sin\theta_{21}^0(-\cos\phi_{21}^0) \\ \cos\theta_{21}^0 \end{bmatrix} . \tag{A2}$$

Since in step (ii) $u,v\to 0$, we only need $w(t=\theta/\alpha)$, so that we get a new initial condition for the second part of the rf pulse [step (iii)]:

$$\mathbf{R}=L_0\begin{bmatrix} 0 \\ 0 \\ \sin\phi_{21}^0\sin\theta_{21}^0\sin\phi\sin\theta+\cos\phi_{21}^0\sin\theta_{21}^0\cos\phi\sin\theta+\cos\theta_{21}^0\cos\theta \end{bmatrix} . \tag{A3}$$

In step (iii), a $2\pi-\theta$ pulse is applied. This yields

$$\begin{aligned}\mathbf{R}&=L_0\begin{bmatrix} -w(t=\theta/\alpha)\sin\phi\sin(2\pi-\theta) \\ w(t=\theta/\alpha)\cos\phi\sin(2\pi-\theta) \\ w(t=\theta/\alpha)\cos(2\pi-\theta) \end{bmatrix} \\ &=L_0a\begin{bmatrix} \sin\phi\sin\theta \\ (-\cos\phi)\sin\theta \\ \cos\theta \end{bmatrix} ,\end{aligned} \tag{A4}$$

with

$$\begin{aligned}a&=(\sin\phi_{21}^0\sin\theta_{21}^0\sin\phi\sin\theta+\cos\phi_{21}^0\sin\theta_{21}^0\cos\phi\sin\theta \\ &\quad+\cos\theta_{21}^0\cos\theta) \\ &=\cos\Delta\phi\sin\theta_{21}^0\sin\theta+\cos\theta_{21}^0\cos\theta .\end{aligned} \tag{A5}$$

[1] N. van Kampen, Physica A **153**, 97 (1988).
[2] Y. Aharonov and M. Vardi, Phys. Rev. D **21**, 2235 (1980).
[3] B. Misra and E. C. G. Sudarshan, J. Math. Phys. **18**, 756 (1977).
[4] C. B. Chiu, E. C. G. Sudarshan, and B. Misra, Phys. Rev. D **16**, 520 (1977).
[5] A. Peres, Am. J. Phys. **48**, 931 (1980).
[6] D. Home and M. A. B. Whitaker, J. Phys. A **19**, 1847 (1986).
[7] E. Joos, Phys. Rev. D **29**, 1626 (1984).
[8] G. C. Ghiradi, C. Omero, T. Weber, and A. Rimini, Nuovo Cimento **52A**, 421 (1979).
[9] E. Block and P. R. Berman, Phys. Rev. A **44**, 1466 (1991).
[10] V. Frerichs and A. Schenzle, Phys. Rev. A **44**, 1962 (1991).
[11] R. J. Cook, Phys. Scr. **T21**, 49 (1988).
[12] W. M. Itano, D. J. Heinzen, J. J. Bollinger, and D. J. Wineland, Phys. Rev. A **41**, 2295 (1990).
[13] P. Meystre and M. Sargent III, *Elements of Quantum Optics* (Springer, Berlin, 1990), Chap. 4.
[14] C. Cohen-Tannoudji, in *Frontiers of Laser Spectroscopy,* edited by R. Balian, S. Haroche, and S. Liberman (North-Holland, Amsterdam, 1977), p. 4.